Preparation and Characterization of a Neutral π-Radical Molecular Conductor

T. M. Barclay,[1a] A. W. Cordes,[1a] R. C. Haddon,[1b] M. E. Itkis,[1b] R. T. Oakley,*[,1c] R. W. Reed,[1c] and H. Zhang[1c]

Contribution from the Department of Chemistry and Biochemistry, University of Arkansas, Fayetteville, Arkansas 72701, Department of Chemistry and Physics, and Advanced Carbon Materials Center, University of Kentucky, Lexington, Kentucky 40506, and Department of Chemistry, University of Waterloo, Waterloo, Ontario N2L 3G1, Canada

Received October 2, 1998

Abstract: The synthesis and solid-state characterization of the heterocyclic π-radical 1,2,5-thiadiazolo[3,4-*b*]-1,2,3-dithiazolo[3,4-*b*]pyrazin-2-yl, 1,2,3-TDTA, is described. The ESR spectrum of 1,2,3-TDTA (in CH_2Cl_2, 293 K, $g = 2.009$) confirms a highly delocalized spin distribution, with observable hyperfine coupling to all five nitrogen atoms of the tricyclic molecule ($a_N = 0.514$, 0.343, 0.109, 0.051, and 0.045 mT). While chemical and electrochemical oxidation ($E_{1/2}$(ox) = 1.14 V vs SCE) of 1,2,3-TDTA requires relatively harsh conditions, reduction is extremely facile ($E_{1/2}$(red) = 0.15 V vs SCE). More importantly both the observed cell potential E_{cell} and computed (MNDO) gas-phase enthalpy ΔH_{disp} for the disproportionation of this and other 1,2,3-dithiazolyls are significantly lower than those observed for their 1,3,2-isomers. Crystals of 1,2,3-TDTA are monoclinic $P2_1/n$, with $a = 6.6749(16)$ Å, $b = 11.7178(14)$ Å, $c = 8.6148(14)$ Å, $\beta = 103.297(16)°$, and $Z = 4$. The crystal structure consists of slipped stacks of head-to-tail (centrosymmetric) π-dimers. The closest intradimer S- - -S contact (S2- - -S3) is 3.2331(15) Å. Variable-temperature magnetic susceptibility measurements establish that 1,2,3-TDTA is essentially diamagnetic at room temperature. The magnetic data, along with the results of variable-temperature single-crystal conductivity measurements (1,2,3-TDTA exhibits a room-temperature conductivity $\sigma = 1 \times 10^{-4}$ S cm^{-1}), are interpreted in terms of one-dimensional hopping mechanism for charge transport.

Introduction

The idea[2] of using neutral π-radicals as building blocks for molecular conductors holds both appeal and challenge. In our pursuit of this goal we have prepared and characterized a wide range of heterocyclic thiazyl radicals.[3] Early work focused on mono-,[4] di-,[5] and trifunctional[6] derivatives of the 1,2,3,5-dithiadiazolyl or DTDA system **1** (Chart 1). Most DTDA radicals associate in the solid state, often forming elegantly stacked π-dimer arrays. While the tendency to dimerize can be reduced by steric bulk,[7] the high electronegativity of the constituent atoms leads to a high Coulombic barrier to charge transfer between adjacent radicals in the solid state. Essentially the spins are trapped on the sites and, while interesting magnetic effects have been reported,[7] DTDA-based materials are Mott insulators. The on-site repulsion *U*, which can be loosely equated with the gas-phase disproportionation enthalpy ΔH_{disp} and the corresponding solution based cell potential E_{cell},[8] can be

Chart 1

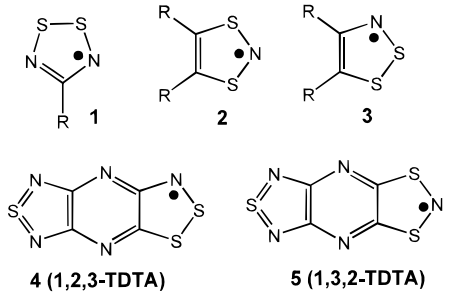

(1) (a) University of Arkansas. (b) University of Kentucky. (c) University of Waterloo.

(2) (a) Haddon, R. C. *Nature (London)* **1975**, *256*, 394. (b) Haddon, R. C. *Aust. J. Chem.* **1975**, *28*, 2343.

(3) (a) Cordes, A. W.; Haddon, R. C.; Oakley, R. T. In *The Chemistry of Inorganic Ring Systems*; Steudel, R., Ed.; Elsevier: Amsterdam, 1992; p 295. (b) Cordes, A. W.; Haddon, R. C.; Oakley, R. T. *Adv. Mater.* **1994**, *6*, 798.

(4) (a) Cordes, A. W.; Haddon, R. C.; Hicks, R. G.; Oakley, R. T.; Palstra, T. T. M. *Inorg. Chem.* **1992**, *31*, 1802. (b) Cordes, A. W.; Bryan, C. D.; Davis, W. M.; de Laat, R. H.; Glarum, S. H.; Goddard, J. D.; Haddon, R. C. Hicks, Kennepohl, D. K.; Oakley, Scott, S. R. Westwood, N. P. C. *J. Am. Chem. Soc.* **1993**, *115*, 7232.

(5) (a) Cordes, A. W.; Haddon, R. C.; Hicks, R. G.; Oakley, R. T.; Palstra, T. T. M.; Schnemeyer, L. F.; Waszczak, J. V. *J. Am. Chem. Soc.* **1992**, *114*, 1729. (b) Cordes, A. W.; Haddon, R. C.; Hicks, R. G.; Kennepohl, D. K.; Oakley, R. T.; Palstra, T. T. M.; Schneemeyer, L. F.; Scott, S. R.; Waszczak, J. V. *Chem. Mater.* **1993**, *5*, 820. (c) Bryan, C. D.; Cordes, A. W.; Goddard, J. D.; Haddon, R. C.; Hicks, R. G.; MacKinnon, C. D.; Mawhinney, R. C.; Oakley, R. T.; Palstra, T. T. M.; Perel, A. S. *J. Am. Chem. Soc.* **1996**, *118*, 330.

(6) (a) Cordes, A. W.; Haddon, R. C.; Hicks, R. G.; Oakley, R. T.; Palstra, T. T. M.; Schneemeyer, L. F.; Waszczak, J. V. *J. Am. Chem. Soc.* **1992**, *114*, 5000. (c) Cordes, A. W.; Haddon, R. C.; Hicks, R. G.; Kennepohl, D. K.; Oakley, R. T.; Schneemeyer, L. F.; Waszczak, J. V. *Inorg. Chem.* **1993**, *32*, 1554.

(7) (a) Banister, A. J.; Bricklebank, N.; Lavender, I.; Rawson, J. M.; Gregory, C. I.; Tanner, B. K.; Clegg, W.; Elsegood, M. R. J.; Palacio, E F. *Angew. Chem., Int. Ed. Engl.* **1996**, *35*, 2533. (b) Banister, A. J.; Bricklebank, N.; Clegg, W.; Elsegood, M. R. J.; Gregory, C. I.; Lavender, I.; Rawson, J. M.; Tanner, B. K. *J. Chem. Soc., Chem. Commun.* **1995**, 679.

(8) ΔH_{disp} is the enthalpy change for the gas-phase reaction $R \rightleftarrows R^+ + R^-$ E_{cell} is defined as the difference in the half-wave potentials for oxidation and reduction, i.e., $E_{cell} = E_{1/2}(ox) - E_{1/2}(red)$.

10.1021/ja983490s CCC: $18.00
Published on Web 01/20/1999

diminished by p-type doping of the half-filled energy band, a change which also renders the uniform structure stable with respect to dimerization.[9] Highly conductive materials have been made in this way. However, for purely neutral systems, the need to design alternative building blocks with lower ΔH_{disp} and E_{cell} values is inescapable.[10,11]

We thus turned to the study of 1,3,2-dithiazolyl (1,3,2-DTA) radicals **2**,[12,13] a family of heterocycles known with a wide range of substituents in the 4,5-positions.[14−17] The appealing feature of the 1,3,2-DTA ring system is that its redox properties can be significantly altered by the electron withdrawing/releasing power of the attached 4,5-substituents; variations in oxidation and reduction potentials of almost 1 V can be induced. More importantly, the cell potentials E_{cell} and disproportionation energies ΔH_{disp} can be significantly reduced relative to those found for DTDAs.[13] However, despite these improvements in charge correlation effects, and also the encouraging observation that evenly spaced (undimerized) slipped stacks of π-radicals can be generated,[12] conductivity remains low ($\sigma_{RT} < 10^{-6}$ S cm^{-1}), even for the best 1,3,2-DTAs.[12,13] Orbital interactions between adjacent radicals along the stacks are still insufficient to offset the Coulombic barrier to charge transport, and the materials remain Mott insulators.

In an attempt to design heterocyclic radicals with still lower $E_{cell}/\Delta H_{disp}$ values, we are now exploring the properties of the isomeric counterparts of 1,3,2-DTAs, i.e., 1,2,3-DTAs **3**. However, while radicals of this type have been known (observed spectroscopically) for many years,[18,19] *none* has ever been isolated and structurally characterized in the solid state. Our first attempt to isolate a simple monocyclic 1,2,3-DTA demonstrated the potential of these radicals to associate irreversibly through carbon.[20] To suppress this C-dimerization problem, while at the same time reducing the $E_{cell}/\Delta H_{disp}$ values as much as possible, we set about the synthesis of 1,2,5-thiadiazolo[3,4-*b*]-1,2,3-dithiazolo[3,4-*b*]pyrazin-2-yl, or 1,2,3-TDTA (**4**). We had previously prepared the isomeric 1,3,2-TDTA (**5**),[13] and preliminary estimates of the ΔH_{disp} value for 1,2,3-TDTA suggested a significant decrease in the charge correlation effect.

Scheme 1

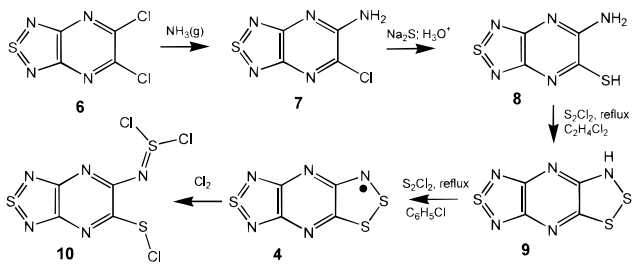

In this paper we report the preparation and solid-state characterization of 1,2,3-TDTA (**4**). The redox properties and ESR spectrum of this radical are compared to those of its 1,3,2-isomer **5**. The crystal structure determination of the dimer of 1,2,3-TDTA constitutes the *first* such characterization of a 1,2,3-dithiazoyl radical. Variable-temperature magnetic susceptibility and single-crystal conductivity measurements on 1,2,3-TDTA have also been performed, and these transport properties are discussed in the light of the design criteria for a neutral radical conductor.

Results and Discussion

Preparation 1,2,3-TDTA. The 5-atom 1,2,3-DTA ring system can be constructed in various ways, including the addition of sulfur monochloride to enamines,[18] and variations on the Herz reaction, i.e., the cyclization of aromatic *ortho*-amino−thiols with sulfur halides.[21] Reduction of the dithiazolylium cation so formed then affords the neutral radical **3**.[22] Although a range of radicals has been well-characterized spectroscopically, nothing is known of the molecular or solid-state structures of these systems. In this work we constructed the target molecule starting from the known compound 5,6-dichloro-1,2,5-thiadiazolo[3,4-*b*]pyrazine (**6**).[23] Monosubstitution of this compound with ammonia, followed by treatment of the resultant amino−chloro derivative **7** with sodium sulfide, then afforded the amino−thiol **8** (Scheme 1). Final cyclization of the latter with excess S_2Cl_2 in refluxing dichlorethane yielded the imide 1,2,3-TDTAH (**9**). The conversion of this imide into the radical proved a challenging task. On one hand we were unable to oxidize **9** to **4** with either bromine or sulfuryl chloride, while on the other we found that chlorine was too harsh an oxidant, causing secondary cleavage of the S−S bond and formation of the trichloro-derivative 1,2,3-TDTACl_3 (**10**). While reduction of the latter with bromide ion could be used to backtrack to the neutral radical, we eventually discovered the

(9) (a) Bryan, C. D.; Cordes, A. W.; Haddon, R. C.; Hicks, R. G.; Kennepohl, D. K.; MacKinnon, Oakley, R. T.; Palstra, T. T. M.; Perel, A. S.; Scott, S. R.; Schneemeyer, L. F.; Waszczak, J. V. *J. Am. Chem. Soc.* **1994**, *116*, 1205. (b) Bryan, C. D.; Cordes, A. W.; Fleming, R. M.; George, N. A.; Glarum, S. H.; Haddon, R. C.; MacKinnon, C. M.; Oakley, R. T.; Palstra, T. T. M.; Perel, A. S.; Schneemeyer, L. F.; Waszczak, J. V. *J. Am. Chem. Soc.* **1995**, *117*, 6880. (c) Bryan, C. D.; Cordes, A. W.; Goddard, J. D.; Haddon, R. C.; Hicks, R. G.; MacKinnon, C. D.; Mawhinney, R. C.; Oakley, R. T.; Palstra, T. T. M.; Perel, A. S. *J. Am. Chem. Soc.* **1996**, *118*, 330.

(10) Boeré, R. T.; Moock, K. H. *J. Am. Chem. Soc.* **1995**, *117*, 4755.

(11) Chandrasekhar, V.; Chivers, T.; Parvez, M.; Vargas-Baca, I.; Ziegler, T. *Inorg. Chem.* **1997**, *36*, 4772.

(12) Barclay, T. M.; Cordes, A. W.; George, N. A.; Haddon, R. C.; Oakley, R. T.; Palstra, T. T. M.; Patenaude,G. W.; Reed, R. W.; Richardson, J. F.; Zhang, H. *J. Chem. Soc., Chem. Commun.* **1997**, 873.

(13) Barclay, T. M.; Cordes, A. W.; George, N. A.; Haddon, R. C.; Itkis, M. E.; Mashuta, M. S.; Oakley, R. T.; Patenaude, G. W.; Reed, R. W.; Richardson, J. F.; Zhang, H. *J. Am. Chem. Soc.* **1998**, *120*, 352.

(14) (a) Preston, K. F.; Sutcliffe, L. H. *Magn. Reson. Chem.* **1990**, *28*, 189. (b) Chung, Y.-L.; Fairhurst, S. A.; Gillies, D. G.; Preston, K. F.; Sutcliffe, L. H. *Magn. Reson. Chem.* **1992**, *30*, 666.

(15) (a) Awere, E. G.; Burford, N.; Mailer, C.; Passmore, J.; Schriver, M. J.; White, P. S.; Banister, A. J.; Oberhammer, A. J.; Sutcliffe, L. H. *J. Chem. Soc., Chem. Commun.* **1987**, 66. (b) MacLean, G. K.; Passmore, J.; Rao, M. N. S.; Schriver, M. J.; White, P. S. *J. Chem. Soc., Dalton Trans.* **1985**, 1405. (c) Wolmershäuser, G.; Kraft, G. *Chem. Ber.* **1989**, *122*, 385. (d) Harrison, S. R.; Pilkington, R. S.; Sutcliffe, L. H. *J. Chem. Soc., Faraday Trans. 1*, **1984**, *80*, 669. (f) Fairhurst, S. A.; Pilkington, R. S.; Sutcliffe, L. H. *J. Chem. Soc., Faraday Trans.* 1 **1983**, *79*, 439. (g) Fairhurst, S. A.; Pilkington, R. S.; Sutcliffe, L. H. *J. Chem. Soc., Faraday Trans. 1* **1983**, *79*, 925.

(16) (a) Wolmershäuser, G.; Kraft, G. *Chem. Ber.* **1990**, *123*, 881. (b) Heckmann, G.; Johann, R.; Kraft, G.; Wolmershäuser, G. *Synth. Met.* **1991**, *41*−*43*, 3287. (c) Wolmershäuser, G.; Johann, R. *Angew. Chem., Int. Ed. Engl.* **1989**, *28*, 920.

(17) (a) Awere, E. G.; Burford, N.; Haddon, R. C.; Parsons, S.; Passmore, J.; Waszczak, J. V.; White, P. S. *Inorg. Chem.* **1990**, *29*, 4821. (b) Wolmershäuser, G.; Schnauber, M.; Wilhelm, T. *J. Chem. Soc., Chem. Commun.* **1984**, 573.

(18) Mayer, R.; Domschke, G.; Bleisch, S.; Bartl, A. *Z. Chem.* **1981**, *21*, 324.

(19) (a) Mayer, R.; Domschke, G.; Bleisch, S. *Tetrahedron Lett.* **1978**, 4003. (b) Mayer, R.; Domschke, G.; Bleisch, S.; Bartl, A.; Stăsko, A. *Z. Chem.* **1981**, *21*, 146, 265. (c) Mayer, R.; Domschke, G.; Bleisch, S.; Fabian, J.; Bartl, A.; Stăsko, A. *Collect. Czech. Chem. Commun.* **1984**, *49*, 684. Mayer, R.; Bleisch, S.; Domschke, G.; Tkáč, A.; Stăsko, A. *Org. Magn. Reson.* **1979**, *12*, 532.

(20) Barclay, T. M.; Cordes, A. W.; Oakley, R. T.; Preuss, K. E.; Reed, R. W. *J. Chem. Soc., Chem. Commun.* **1998**, 1039.

(21) Warburton, W. K. *Chem. Rev.* **1957**, *57*, 1011.

(22) Barclay, T. M.; Cordes, A. W.; Goddard, J. D.; Mawhinney, R. C.; Oakley, R. T.; Preuss, K. E.; Reed, R. W. *J. Am. Chem. Soc.* **1997**, *119*, 12136.

(23) Tong, Y. C. *J. Heterocycl. Chem.* **1975**, *12*, 451.

Table 1. Half-Wave Redox and E_{cell} Potentials[a] (V vs SCE) and Computed (MNDO) IP, EA, and ΔH_{disp} Values (eV) for 1,3,2- and 1,2,3-Dithiazolyls

	compound			
param	1,3,2-BDTA	1,3,2-TDTA	1,2,3-BDTA	1,2,3-TDTA
$E_{1/2}$(ox)	0.15	1.00	0.18	1.14
$E_{1/2}$(red)	−1.24[b]	−0.06	−1.0[b]	0.15
E_{cell}[c]	1.33[d]	1.06	1.15[d]	0.99
IP	7.81	8.55	7.86	8.92
EA	1.45	3.02	2.44	4.03
ΔH_{disp}	6.36	5.53	5.41	4.88

[a] All potentials are from solutions in CH_3CN, reference SCE. [b] Irreversible. [c] E_{cell} defined as the difference in the half-wave potentials for oxidation and reduction, i.e., $E_{cell} = E_{1/2}(ox) - E_{1/2}(red)$. [d] This value taken as the difference in the cathodic peak potentials, since the reduction wave is irreversible.

simplest and most effective method for the conversion of **9** to **4** involved the use of sulfur monochloride in refluxing chlorobenzene. In this way, starting from either **8** or **9**, we could generate **4** in good yield. The radical, isolated as a lustrous black crystalline solid, was purified by fractional sublimation in vacuo.

Redox Chemistry. The thiadiazolopyrazine (TDP) ligand serves as a powerful electron-withdrawing ligand when attached to a 1,3,2-DTA radical **2**. Thus the redox potentials of 1,3,2-TDTA experience dramatic anodic shifts (Table 1) in comparison to the simple benzo-derivative 1,3,2-BDTA (**11**). Computed

11 (1,3,2-BDTA) **12 (1,2,3-BDTA)**

(MNDO) estimates of IPs and EAs follow suit.[24] In the context of molecular conductor design, the favorable shifts in EA and $E_{1/2}$(red) outpace the more adverse changes in IP and $E_{1/2}$(ox). The net effect is thus a diminution in both ΔH_{disp} and E_{cell} and an evolution toward a system with a lower barrier to charge transfer in the solid state.[2]

Initial MNDO calculations on model 1,2,3-DTA rings suggested that they should provide better charge-transfer characteristics relative to their 1,3,2- counterparts. As indicated in Table 1, the computed ΔH_{disp} values of both 1,2,3-BDTA (**12**) and 1,2,3-TDTA are smaller than those seen in the 1,3,2-series, largely as a result of the higher electron affinity for the 1,2,3-ring. The results of cyclic voltammetric (CV) analysis measurements on 1,2,3-BDTA[25] and 1,2,3-TDTA support these theoretical predictions. The reversible oxidation and reduction waves for the two 1,2,3-TDTA isomers are illustrated in Figure 1. In accord with its chemical behavior, notably the difficulty experienced in accessing the neutral radical from its imide **9**, the electrochemical reduction of 1,2,3-TDTA occurs at 0.15 V vs SCE, a potential similar to that found for strong closed-shell acceptors, e.g., TCNQ (0.127 V).[26] Oxidation also requires more forcing conditions, and most importantly, the overall cell potential E_{cell} is reduced from 1.06 V in the 1,3,2-isomer to 0.99 V in the 1,2,3-compound, the lowest value we have ever observed for a heterocyclic thiazyl radical.

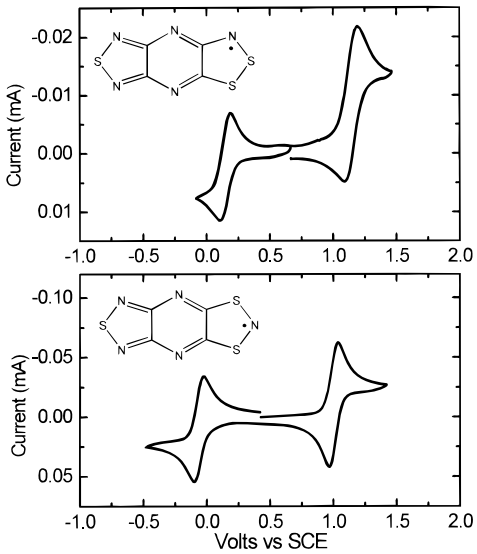

Figure 1. Cyclic voltammetry waves on 1,2,3-TDTA and 1,3,2-TDTA radicals (in CH_3CN, n-Bu_4NPF_6 supporting electrolyte, reference SCE).

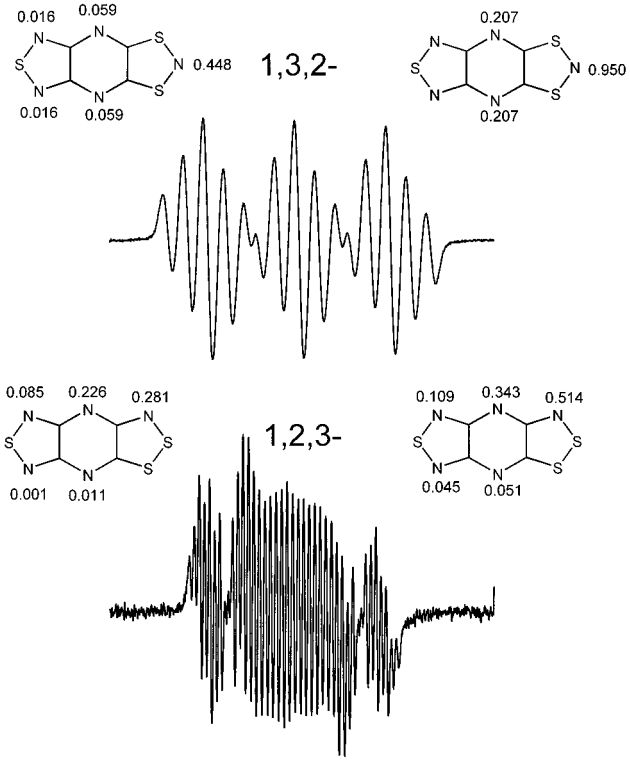

Figure 2. X-Band ESR spectra of 1,2,3-TDTA and 1,3,2-TDTA (in CH_2Cl_2, 293 K, sweep width 4 mT). Derived ^{14}N hyperfine coupling constants a_N are shown on the right, and calculated (MNDO) spin densities $q\pi$ are shown on the left.

ESR Spectra. The X-band ESR spectra (in CH_2Cl_2, 293 K) of the two TDTA isomers are shown in Figure 2. The signal ($g = 2.009$) of the 1,2,3-derivative is considerably more complex, but spectral simulation reveals the effects of hyperfine coupling to all five nitrogen nuclei. The assignments of the derived a_N values are provided in Figure 2, along with the calculated (MNDO) spin densities $q\pi$ for both systems. The results reveal that while the thiadiazolopyrazine (TDP) residue simply refines the spin distribution of a 1,3,2-DTA radical, it causes a major reorganization of the electronic structure of a 1,2,3-DTA radical.

(24) For 1,3,2-BDTA we also have ab initio estimates of the IP and EA, along with experimental IPs from its UV photoelectron spectrum. The MNDO estimates presented here provide self-consistency with the other calculated IP and EA values. See: Barclay, T. M.; Cordes, A. W.; de Laat, R. H.; Goddard, J. D.; Haddon, R. C.; Jeter, D. Y.; Mawhinney, R. C.; Oakley, R. T.; Palstra, T. T. M.; Patenaude, G. W.; Reed, R. W.; Westwood, N. P. C. *J. Am. Chem. Soc.* **1997**, *119*, 2633.

(25) Cyclic voltammetry on the 1,2,3-BDTA system has been reported by Tsveniashvili, V. Sh.; Malashkiya, M. V. *Electrokhimiya* **1984**, *3*, 357. The data provided in Table 1 refer to measurements made in our laboratories.

(26) Bard, A. J.; Faulkner, L. R. In *Electrochemical Methods*; J. Wiley and Sons: New York, 1980; Appendix C.

Table 2. Crystal Data for 1,2,3-TDTA (**4**) and 1,2,3-TDTACl_3 (**10**)

compd	**4**	**10**
formula	$S_3N_5C_4$	$S_3N_5C_4Cl_3$
fw	214.26	320.61
a, Å	6.6749(16)	8.6990(11)
b, Å	11.7178(14)	6.8203(17)
c, Å	8.6148(14)	9.4167(10)
β, deg	103.297(16)	111.261(9)
V, Å^3	655.7(2)	520.67(16)
space group	$P2_1/n$	$P2_1/m$
Z	4	2
temp, K	293	293
μ, mm^{-1}	1.02	1.43
data with $I > 1.0\sigma(I)$	1010	857
params refined	109	89
$R(F)$, $R_w(F)^a$	0.037, 0.050	0.031, 0.036

[a] $R = [\sum||F_o| - |F_c||]/[\sum|F_o|]$; $R_w = \{[\sum w||F_o| - |F_c||^2]/[\sum(w|F_o|^2)]\}^{1/2}$.

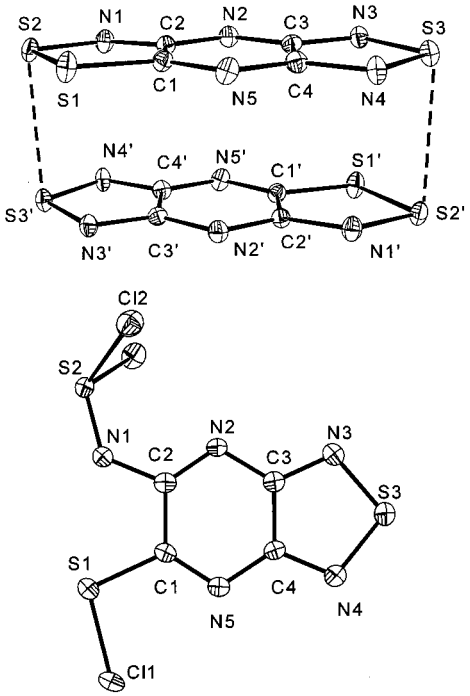

Figure 3. ORTEP drawings of a single dimer unit in 1,2,3-TDTA (top) and compound **10** (bottom), showing the atom numbering.

In simple monofunctional 1,2,3-DTA radicals spin density is heavily localized at the 4-position of the heterocycle; i.e., they are carbon-centered radicals.[20] By contrast, in 1,2,3-TDTA, spin density is stripped away from the 5-position and is redistributed not only to the nitrogen attached to the 4-position of the DTA ring but also to the other three nitrogens of the TDP ligand. As a result of this reorganization of spin density, the 1,2,3-TDTA radical resists association via C−C bond formation.

Crystal Structures. We have determined two crystal structures in the course of this work. That of the oxidized derivative 1,2,3-TDTACl_3 (**10**) was performed in order to confirm its structural identity and also to provide a basis for comparison with the radical 1,2,3-TDTA itself. Crystal data for the two compounds are provided in Table 2. An ORTEP drawing of 1,2,3-TDTA, showing the atom numbering, is shown in Figure 3. Table 3 provides the atomic parameters for 1,2,3-TDTA, while Table 4 summarizes the intramolecular distances in 1,2,3-TDTA and 1,2,3-TDTACl_3.

Crystals of 1,2,3-TDTA belong to the monoclinic space group $P2_1/n$; there are four radical molecules per unit cell. The radicals,

Table 3. Atomic Parameters *x*, *y*, and *z* and B_{eq} Values (Å^2) for 1,2,3-TDTA (**4**)

	x	*y*	*z*	B_{eq}[a]
S1	0.67752(15)	0.22234(8)	0.16892(10)	2.51(4)
S2	0.70755(14)	0.31574(8)	0.37396(10)	2.14(4)
S3	0.75159(14)	0.58467(8)	−0.34348(10)	2.16(4)
N1	0.7383(4)	0.4409(2)	0.3062(3)	2.02(13)
N2	0.7683(4)	0.5469(2)	0.0842(3)	1.82(11)
N3	0.7837(4)	0.6309(2)	−0.1619(3)	1.89(12)
N4	0.7066(5)	0.4483(2)	−0.3216(3)	2.11(12)
N5	0.6876(4)	0.3341(2)	−0.0966(3)	2.03(12)
C1	0.7014(5)	0.3415(3)	0.0577(4)	1.77(13)
C2	0.7378(5)	0.4471(3)	0.1506(4)	1.68(13)
C3	0.7576(5)	0.5396(3)	−0.0735(4)	1.62(12)
C4	0.7151(5)	0.4349(3)	−0.1650(4)	1.78(13)

[a] B_{eq} is the mean of the principal axes of the thermal ellipsoid.

Table 4. Intramolecular Distances (Å) in 1,2,3-TDTA (**4**) and 1,2,3-DTDACl_3 (**10**)

	4	**10**		**4**	**10**
S1−S2	2.0482(13)		N2−C3	1.347(4)	1.369(5)
S1−C1	1.721(3)	1.754(4)	N3−C3	1.347(4)	1.335(5)
S2−N1	1.609(3)	1.516(3)	N4−C4	1.347(4)	1.333(5)
S3−N3	1.622(3)	1.618(4)	N5−C1	1.314(4)	1.301(5)
S3−N4	1.644(3)	1.619(4)	N5−C4	1.351(4)	1.364(5)
N1−C2	1.342(4)	1.403(5)	C1−C2	1.463(5)	1.451(5)
N2−C2	1.338(4)	1.293(5)	C3−C4	1.450(5)	1.417(6)

which are planar to within 0.07 Å, are loosely associated into centrosymmetric or head-to-tail dimers (Figure 3), the closest intradimer S- - -S contact d_1 (=S2- - -S3) being 3.2331(15) Å. This distance is shorter than the interannular contacts observed in the low-temperature phase of 1,3,2-TDTA[13] but longer than those seen in the dimer of 1,3,2-BDTA.[17a] As the magnetic measurements (vide infra) indicate, interannular orbital interactions at this range are weak but sufficient to quench paramagnetism, i.e., to generate a weak "chemical bond" between the two radicals. Within the individual halves of the dimer the bond lengths show changes from those seen in compound **10** that reflect the long-range nature of the electron delocalization in the radical. The shortening of the N1−C2 bond relative to 1,2,3-TDTACl_3 heralds considerable double bond character. This change, coupled with the shortening of N2−C3 and N5−C4, and the lengthening of N2−C2, suggest the collective involvement of the series of valence bond resonance structures **4A**−**C**.

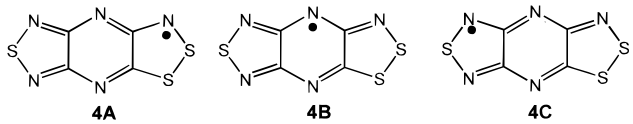

Several views of the packing of the dimers are shown in Figure 4. The dimers adopt a slipped π-stack motif within which the closest interdimer S- - -S separation d_2 (=S2- - -S3′) is 3.8601(15) Å. In addition to these intrastack contacts there are two interstack S- - -S contacts d_3 (=3.5819(15) Å) and d_4 (=3.3610(13) Å) that are within the van der Waals approach (3.6 Å) for two sulfurs.[27]

Magnetic Measurements. The magnetic susceptibility of 1,2,3-TDTA (**4**) has been measured over the temperature range 5−380 K, and the results are plotted in Figure 5. The compound is essentially diamagnetic. In the low-temperature regime the susceptibility exhibits a Curie−Weiss dependence (solid line in Figure 5a), with a derived diamagnetic contribution χ_0 =

(27) Bondi, A. *J. Phys. Chem.* **1964**, *68*, 41.

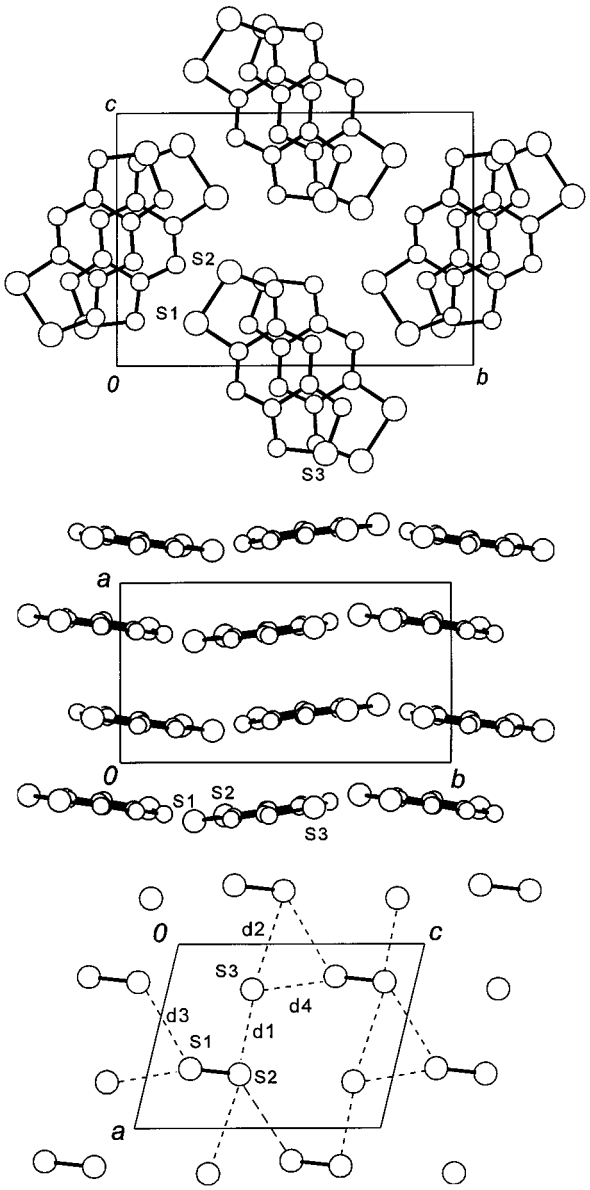

Figure 4. Packing of 1,2,3-TDTA, shown from above and the side. The four intermolecular distances (dashed lines) are $d_1 = 3.2331(15)$, $d_2 = 3.8601(15)$, $d_3 = 3.5819(15)$, and $d_4 = 3.3610(13)$ Å.

-133×10^{-6} emu mol^{-1}, a Θ value of 6.4 K, and a residual spin concentration of 0.2% (Figure 5b). Above 200 K a deviation $\Delta\chi$ from Curie−Weiss behavior is observed (Figure 5a) in the form of an enhanced paramagnetism which reaches a value that corresponds to 2% of the molecules carrying free Curie spins at 380 K (Figure 5b). This enhancement $\Delta\chi$ shows an activated temperature dependence (see the plot of $\Delta\chi$ vs $1/T$ in Figure 5c) with activation energy $\Delta = 2000$ K (0.17 eV). Similar paramagnetic enhancements of larger magnitude have been observed in the structures of dithiadiazolyl π-dimer stacks,[5,28] and this behavior has been attributed to an uncoupling of the weak intradimer bonds and the formation of spin defects in the lattice. Such spin uncoupling can clearly also take place at elevated temperatures in 1,2,3-TDTA, but it is interesting, in view of the weakness of the interannular interactions (as evidenced by the molecular separation), that the degree of uncoupling is so small.

Conductivity Measurements. The single-crystal conductivity (σ) of 1,2,3-TDTA was measured in a four probe configuration. The in-line contacts were made with silver paint. The crystal

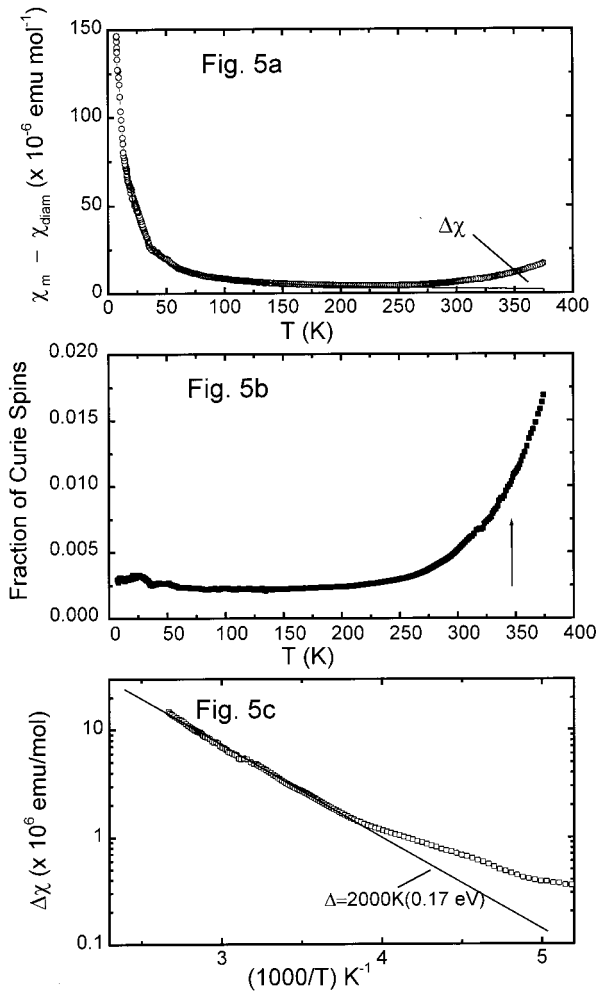

Figure 5. (a) Magnetic susceptibility $\chi_M - \chi_0$ of solid-state 1,2,3-TDTA as a function of temperature, (b) fraction of Curie spins as a function of T, and (c) $\Delta\chi$ as a function of $1/T$.

dimensions were $1 \times 0.3 \times 0.3$ mm^3. The temperature dependence of the conductivity was measured in the range 345−75 K. At 75 K the sample resistance was over 10^{13} Ω, the limit of the experimental setup. The high-temperature limit was set by the sample degradation that appeared above 345 K as an irreversible increase in the sample resistance. The results are shown in Figure 6a. The conductivity decreases by 8 orders of magnitude with decreasing temperature from 345 to 75 K. The Arrhenius plot of the same data (Figure 6b) shows activated behavior for σ with variable activation energy, the characteristic feature of hopping conductivity.[29] Near room temperature the activation energy Δ is about 2600 K (0.22 eV), which is close to the activation energy of the free Curie spins (Figure 5c) and is consistent with a gap value $2\Delta = 0.4$ eV calculated in the next section. This correlation suggests that the thermally released free spins are the same carriers which contribute to the conductivity. Figure 6c shows that the temperature dependence of the logarithm of conductivity is proportional to $T^{-1/2}$, as predicted for one-dimensional variable range hopping.[30,31] The three- and two-dimensional variable-range hopping theories[29]

(28) Beekman, R. A.; Boeré, R. T.; Moock, K. H.; Parvez, M. *Can. J. Chem.* **1998**, *76*, 85.
(29) Mott, N. F.; Davis, E. A. *Electronic Processes in Non-Crystalline Materials*; Oxford University Press: New York, 1979.
(30) Shante, V. K. S.; Varma, C. M.; Bloch, A. N. *Phys. Rev.* **1973**, *B8*, 4885.
(31) Brenig, W.; Dohler, G. H.; Heyszenau, H. *Philos. Mag.* **1973**, *27*, 1093.

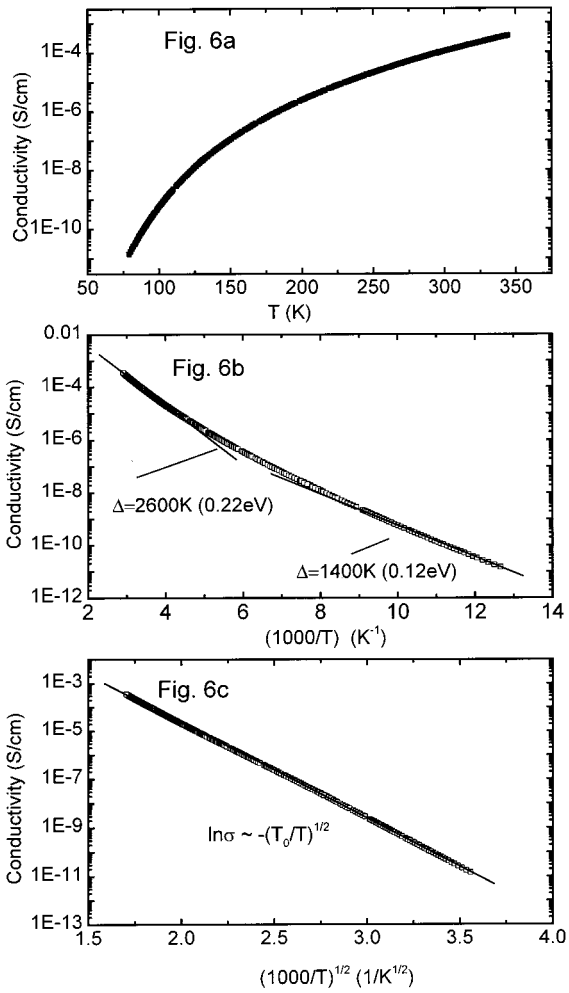

Figure 6. Conductivity of solid-state 1,2,3-TDTA, plotted as a function of (a) absolute temperature T, (b) $1/T$, and (c) $(1/T)^{1/2}$.

($T^{-1/4}$ and $T^{-1/3}$ dependencies, respectively) do not fit to our data. The observed behavior of the conductivity suggests that defect states exist within the gap near the Fermi level and at least at low temperature the transport is dominated by variable-range hopping involving these states. The transport is preferentially one-dimensional in the *x*-direction along the molecular stacks. At high temperatures the hopping would involve states near the gap edge, $\Delta = 2600$ K, where the carrier mobility is higher.

Band Structure Calculations. To probe the extent of intermolecular orbital interactions in 1,2,3-TDTA, we have performed extended Hückel band structure calculations on the full solid-state structure. Figure 7 illustrates the dispersion curves of the highest lying occupied and lowest lying unoccupied molecular orbitals, plotted along the three principal directions of reciprocal space. As expected from the magnetic measurements, dimerization of the radicals leads to the opening of a band gap at the Fermi level, leading to a closed-shell semiconducting state. The calculations suggest the band gap is ca. 0.4 eV, a value considerably smaller than that found in other radical dimer structures we have studied, and consistent with the magnetic and conductivity data reported above. The small size of the band gap cannot be ascribed to crystal orbital dispersion along the stacking direction.[32] Rather, the small valence/

(32) Given that the unit cell angles are equal to or close to 90°, and that there is a close correspondence between real and reciprocal space vectors, orbital dispersion along *a**, *b**, and c* can be equated with orbital interactions parallel to *x*, *y*, and *z*.

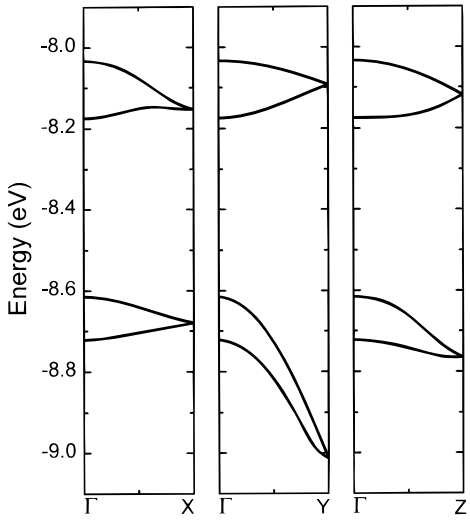

Figure 7. Dispersion of the valence and conduction bands of 1,2,3-TDTA.

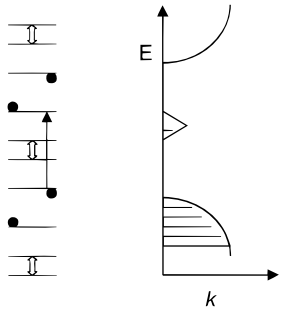

Figure 8. One-dimensional variable range hopping model for solid-state 1,2,3-TDTA. The midgap states arise from topological defects in the lattice and thermal dissociation of dimers.

conduction band splitting arises from the weakness of the *intra*dimer interactions, which we attribute to the unique head-to-tail mode of association. Uncoupling of the dimers will produce defects and midgap states which are important for conductivity (see below), but these cannot be adequately described by the ideal crystal model used for the band calculations.

Conduction Model. The one-dimensional hopping model,[29] as it applies to 1,2,3-TDTA, is summarized in Figure 8. At low temperatures topological defects and some lattice disorder are responsible for the finite density of states within the gap that leads to hopping conductivity. With increasing temperature the free spins that are created by dissociation of the dimers appear as midgap states at the Fermi level. Presumably the same situation arises with the dithiadiazolyl compounds, where a fairly large density of midgap states is generated.[5,28] However these midgap states in the dithiadiazolyls do not contribute to the conductivity and the states are localized—apparently by the large onsite Coulomb correlation energy. Thus we consider the dithiadiazolyls as Mott insulators. The new feature for 1,2,3-TDTA is the identification of enhanced conductivity with these midgap states. Thus these states are not fully localized in 1,2,3-TDTA and they contribute to the conductivity by variable-range hopping. It may be appropriate to view these mid-gap states as separate donor and acceptor bands,[29] because these states will be split by the relatively large Coulomb correlations still remaining in this organic molecule. In this way the conduction in 1,2,3-TDTA would be viewed as arising from one-dimensional variable range hopping involving semimetallic midgap states. In this model the low-temperature conductivity

originates from hopping between midgap states (Figure 6b, $\Delta = 0.12$ eV), whereas at high temperatures the conductivity is mainly associated with hopping that also involves midgap states and the band edges of either the valence or conduction bands ($\Delta = 0.22$ eV, in good agreement with the energy gap of 2Δ, discussed above).

At room temperature σ approaches 1×10^{-4} S cm^{-1}, rising to a value of 4×10^{-4} at 345 K. These values are significantly higher than those observed for 1,3,2-TDTA (**5**) and, indeed, any heterocyclic thiazyl radical or radical dimer system we have yet encountered. We can estimate the mobility μ in 1,2,3-TDTA. Using the observed value of the fraction of free spins (0.5% at room temperature, Figure 5b) and the volume of the molecular unit cell (1.6×10^2 Å^3 mol^{-1}), we obtain a carrier (spin) density $n = 3 \times 10^{19}$ cm^{-3}. Hence $\mu = \sigma/(en) = 2 \times 10^{-5}$ cm^2 V^{-1} s^{-1} at room temperature, a reasonably high value for this class of materials.[33]

Summary and Conclusions

In our pursuit of neutral π-radical conductor materials we faced two fundamental design challenges. First, we have endeavored to suppress the structural (Peierls) instability associated with a half-filled one-dimensional energy band, i.e., the tendency of π-stacked radicals to dimerize. Overcoming the self-association of radicals has required that the radical spins be highly delocalized at the molecular level and that in the solid state two- and three-dimensional intermolecular interactions be enhanced. We have addressed both of these issues by using ring systems in which carbon, along with its exocyclic ligand (even if only a C−H group), is replaced by a heteroatom.

However, while aiding in the resolution of the structural issue the use of heteroatoms creates a second, energetic problem. The extreme electronegativity that results from incorporation of nitrogen and sulfur atoms into the skeletal framework leads to a higher ionization potentials, a trend which is counterproductive to the design of radicals with a low disproportionation enthalpy ΔH_{disp}. Under these circumstances the radical spins become trapped on the molecular building blocks and in the solid state the materials are Mott insulators. The 1,3,2-TDTA radical **5** provides a good example of such a system,[13] i.e., an undimerized π-stacked structure in which the bandwidth is insufficient to overcome the Coulombic barrier U to charge transport.[2] In the isomeric 1,2,3-TDTA radical **4** reported here, U is lowered by virtue of a dramatic increase in electron affinity, one which more than offsets the small increase in ionization potential. However, in the solid state the 1,2,3-TDTA radical does not adopt a simple slipped π-stacked structure but rather a slipped π-dimer stack in which the dimers are coupled in a hitherto unobserved head-to-tail arrangement. As a result of this association the radical spins are paired and a *small* energy gap is opened at the Fermi level. Nonetheless, the resulting material exhibits a remarkably high conductivity. Indeed it is, to our knowledge, the highest conductivity ever observed for a single-component[34] sulfur-based molecular material. More important, however, is the fact that the free spins generated by uncoupling of 1,3,2-TDTA dimers at elevated temperatures contribute to an enhancement in conductivity. We are hopeful that continued exploration of related heterocyclic radicals will lead to materials with even higher conductivities.

(33) Haddon, R. C.; Siegrist, T.; Fleming, R. M.; Bridenbaugh, P. M.; Laudise, R. A. *J. Mater. Res.* **1995**, 1719.

(34) We differentiate our neutral radical materials, which are single component, from highly polarized donor−acceptor compounds. For examples of the latter, see: Yamashita, Y.; Tomura, M. *J. Mater. Chem.* **1998**, *8*, 1933.

Experimental Section

General Procedures and Starting Materials. The reagents chloropyrazine (Aldrich), sodium sulfide (Aldrich), potassium phthalimide (Aldrich), tetra-*n*-butylammonium bromide (Aldrich), sulfur monochloride (Aldrich), and ammonia (Matheson) were obtained commercially and used as received. The compounds tetrachloropyrazine,[35] 2,3-diamino-5,6-dichloropyrazine,[23] and 5,6-dichloro-1,2,5-thiadiazolo[3,4-*b*]pyrazine (**6**),[23] were all prepared by standard literature procedures. Solvents were of reagent grade and dried by distillation from P_2O_5 (for acetonitrile, chlorobenzene, and dichloroethane) and Mg (for EtOH). Crystals of 1,2,3-TDTA suitable for X-ray work were grown by sublimation in an ATS series 3210 three-zone tube furnace mounted horizontally and linked to a series 1400 temperature control system. Melting points are uncorrected. Infrared spectra (Nujol mulls, KBr optics) were recorded on a Nicolet 20SX/C FTIR spectrometer at 2 cm^{-1} resolution. Low-resolution mass spectra (70 eV, EI/DEI and CI/DCI) were run on a Finnigan 4500 quadrupole mass spectrometer at the McMaster Regional Centre for Mass Spectrometry. X-Band ESR spectra were recorded on a Varian E-109 spectrometer with DPPH as a field marker. ESR spectral simulations were accomplished with Win-EPR Simfonia Version 1.25, by Bruker Analytische Messtechnik GmbH. Elemental analyses were performed by MHW Laboratories, Phoenix, AZ 85018.

Preparation of Compound 7. Ammonia gas was passed over a solution of 5,6-dichloro-1,2,5-thiadiazolo[3,4-*b*]pyrazine (**6**) (5.00 g, 24.2 mmol) in 100 mL toluene for 30 min. The gas flow was halted and the mixture left to stir for 1 h at room temperature. The yellow solid was filtered off, washed with 50 mL ether, and sucked dry. The crude product was extracted by boiling with 300 mL of hot toluene (in which the presumed "diamino" derivative and ammonium chloride are insoluble). Hot filtration of the extract and cooling of the filtrate afforded canary yellow needles of **7** (1.88 g, 10.0 mmol, 42%), mp 216−218 °C. Evaporation of the toluene extracts afforded 0.4 g (1.8 mmol) of unreacted **6**. IR: 3419 (m), 3296 (w), 3127 (m, br), 1656 (vs), 1482 (m), 1343 (m), 1107 (s), 925 (w), 872 (m), 817 (m), 783 (w), 642 (m), 536 (vs), 474 (w), 434 (m) cm^{-1}. MS (*m*/*e*): 187 (M$^+$, 100%), 152 (65%), 87 (14%), 74 (18%), 68 (50%), 53 (45%). Anal. Calcd for $C_4H_2N_5SCl$: C, 25.61; H, 1.07; N, 37.33. Found: C, 25.74; H, 0.97; N, 37.50.

Preparation of Compound 8. Anhydrous sodium sulfide (1.84 g, 23.6 mmol) was added to a slurry of **7** (4.00 g, 21.3 mmol) in 80 mL of anhydrous ethanol, and the resulting orange red slurry was stirred under nitrogen for 16 h at 50 °C. Aqueous HCl (100 mL, 10%) was then added to the mixture, and the resulting orange precipitate was filtered off, washed with water and ethanol, and sucked dry. The crude product was recrystallized from boiling benzonitrile (350 mL) as red brown microcrystals of **8** (3.07 g, 16.6 mmol, 78%), subl. > 280 °C. IR: 3402 (m), 3260−3070 (br, m), 1633 (s), 1601 (s), 1576 (s), 1312 (s), 1292 (m), 1126 (s) 852 (m), 806 (s), 778 (m), 693 (s), 516 (w), 467 (m) cm^{-1}. MS (*m*/*e*): 185 (M$^+$, 55%), 112 (21%), 68 (20%), 58 (100%). Anal. Calcd for $C_4H_3N_5S_2$: C, 25.94; H, 1.63; N, 37.81. Found: C, 26.16; H, 1.56; N, 37.73.

Preparation of Compound 9. Excess sulfur monochloride (4 mL) was added to a slurry of amino−thiol (0.50 g, 2.70 mmol) in 35 mL of dichloroethane, and the mixture was stirred and heated at gentle reflux for 6 h. The mixture was cooled and the red microcrystalline solid filtered off, washed with 2 × 20 mL of dichloroethane, and dried in vacuo (0.56 g, 2.62 mmol, 97%). The crude product **9** was purified, for analytical purposes, by fractional sublimation at 140−80 °C/10^{-2} Torr as orange microcrystals, dec > 230 °C. IR: 3188 (w), 1586 (s), 1564 (w), 1318 (s), 1277 (w), 1247 (m), 1079 (w), 838 (w), 828 (w), 785 (s), 717 (m), 693 (w), 508 (m) cm^{-1}. MS (*m*/*e*): 215 (M$^+$, 100%), 84 (11%), 70 (11%), 64 (35%), 46 (26%). Anal. Calcd for $C_4HN_5S_3$: C, 22.32; H, 0.47; N, 32.53. Found: C, 22.54; H, 0.29; N, 32.70.

Preparation of 1,2,3-TDTA (4). Excess sulfur monochloride (6 mL) was added to a slurry of **7** (1.50 g, 8.10 mmol) in 50 mL of chlorobenzene, and the mixture was stirred and heated at reflux for 3 h. The black solid was filtered off, washed with 2 × 20 mL acetonitrile,

(35) Allison, C. G.; Chambers, R. D.; MacBride, J. A. H.; Musgrave, W. K. R. *J. Chem. Soc. C* **1970**, 1023.

and dried in vacuo (0.135 g, 6.31 mmol, 78%). The crude product was purified by slow, fractional sublimation (to remove traces of **9**) at 155−120 °C/10^{-2} Torr in a gradient tube furnace to afford jet black needles, dec > 270 °C. Further purification was effected by a second sublimation at 140−80 °C/10^{-2} Torr in a sealed tube. IR: 1417 (w), 1331 (s), 1293 (m), 1090 (w), 949 (m), 879 (s), 857 (m), 800 (m), 686 (m), 633 (m), 531 (m), 495 (w), 495 (m), 448 (m), 405 (s) cm^{-1}. Anal. Calcd for $C_4N_5S_3$: C, 22.42; N, 32.69. Found: C, 22.53; 32.65.

Preparation of 1,2,3-TDTACl$_3$ (10). Chlorine gas was passed over a slurry of **9** (0.250 g, 1.16 mmol) in 20 mL of CH_3CN. The mixture was gently warmed until all the solid dissolved to afford an orange solution (30 min). Canary yellow needles of 1,2,3-TDTACl$_3$ (**10**) grew upon cooling the solution to −20 °C. These were filtered off under nitrogen, washed with 2 × 5 mL of cold CH_3CN, and pumped dry (yield 0.300 g, 0.94 mmol, 81%), dec > 135 °C. IR: 1521 (m), 1458 (s), 1384 (s), 1293 (s, br), 1246 (m), 1136 (s), 1021 (m) 917 (m), 869 (m), 814 (m), 759 (m), 681 (w), 636 (m), 549 (s), 467 (s), 431 (s) cm^{-1}. Anal. Calcd for $C_4N_5S_3Cl_3$: C, 14.98; N, 21.84. Found: C, 15.10; N, 21.98. Crystals suitable for X-ray work were grown by recrystallization from CH_3CN.

Reduction of 1,2,3-TDTACl$_3$ to 1,2,3-TDTA. Tetra-*n*-butylammonium bromide (1.21 g, 3.75 mmol) was added to a slurry of 1,2,3-TDTACl$_3$ (**10**) (0.400 g, 1.25 mmol) in 20 mL of CH_3CN. After 5 min a black precipitate of 1,2,3-TDTA (215 mg, 1.00 mmol, 80%) was filtered off and dried in vacuo. Its identity was confirmed by comparison of its IR spectrum with that of a known sample.

Cyclic Voltammetry. Cyclic voltammetry was performed on a PAR 273A electrochemical system (EG&G Instruments) with scan rates 50−100 mV s^{-1} on solutions of the radical (0.1 M tetra-*n*-butylammonium hexafluorophosphate) in CH_3CN (dried by distillation from P_2O_5). Measurements on the 1,2,3-BDTA system were made on the PF_6^- salt of the corresponding 1,2,3-BDTA cation. Potentials were scanned from −2.5 to 1.5 V with respect to the quasi-reference electrode in a single compartment cell fitted with Pt electrodes and referenced to the ferrocenium/ferrocene couple at 0.38 V vs SCE.[36]

X-ray Measurements. X-ray data were collected on ENRAF-Nonius CAD-4 with monochromated Mo Kα radiation. Crystals were mounted on glass fibers with silicone or epoxy. Data were collected using a $\theta/2\theta$ technique. The structures were solved using direct methods and refined by full-matrix least squares which minimized $\sum w(\Delta F)^2$.

Magnetic Susceptibility Measurements. Magnetic susceptibilities were measured over the temperature range 5−380 K on a George Associates Faraday balance operating at 0.5 T.

Conductivity Measurements. Conductivity was measured in a helium variable-temperature probe using a LakeShore 340 temperature controller. A Keithley 236 unit was used as a voltage source and current meter, and two 6517A Keithley electrometers were used to measure the voltage drop between the potential leads in a four-probe configuration.

Electronic Structure Calculations. Semiempirical (MNDO) calculations were carried out using the MOPAC93 suite of programs[37] compiled to run under DOS. All geometries were optimized within the constraints of C_{2v} symmetry. Spin densities q_N refer to the square of the pπ-orbital coefficients in the SOMO. The band structure calculations were carried out with the EHMACC suite of programs[38] using the parameters discussed previously.[39] The off-diagonal elements of the Hamiltonian matrix were calculated with the standard weighting formula.[40]

Acknowledgment. We thank the Natural Sciences and Engineering Research Council of Canada, the NSF/EPSCoR program (Grant No. EPS-9452895), the State of Arkansas, the Department of Energy (Grant No. DE-FG02-97ER45668) and the MRSEC program of the NSF (Award No. DMR-9809686) for financial support. We also acknowledge the Department of Education for a doctoral fellowship to T.M.B.

Supporting Information Available: Tables of crystal, structure solution, and refinement data, bond lengths and angles, and anisotropic thermal parameters for the structures reported (PDF). X-ray files, in CIF format, are available. See any current masthead page for Web access instructions.

JA983490S

(36) Boeré, R. T.; Moock, K. H.; Parvez, M. *Z. Anorg. Allg. Chem.* **1994**, *620*, 1589.

(37) MOPAC93, Quantum Chemistry Program Exchange.

(38) EHMACC, Quantum Chemistry Program Exchange, program no. 571.

(39) (a) Cordes, A. W.; Haddon, R. C.; Oakley, R. T.; Schneemeyer, L. F.; Waszczak, J. V.; Young, K. M.; Zimmerman, N. M. *J. Am. Chem. Soc.* **1991**, *113*, 582. (b) Basch, H.; Viste, A.; Gray, H. B. *Theor. Chim. Acta* **1965**, *3*, 458.

(40) Ammeter, J. H.; Burghi, H. B.; Thibeault, J. C.; Hoffmann, R. *J. Am. Chem. Soc.* **1978**, *100*, 3686.